

Comparative Studies on Electronic Structures and Surface Acoustic Wave Properties of (Ca, Sr, Pb)₃Ga₂Ge₃O₁₄ Piezoelectric Crystals

Wenqi Huang¹ & Hong Yang¹

¹ School of Applied Science, Beijing information science & technology university, Beijing, China

Correspondence: Wenqi Huang, School of Applied Science, Beijing information science & technology university, Beijing, China. E-mail: hwq5667@gmail.com

Received: March 11, 2014 Accepted: March 31, 2014 Online Published: April 28, 2014

doi:10.5539/apr.v6n3p90

URL: <http://dx.doi.org/10.5539/apr.v6n3p90>

Abstract

The electronic structural and surface acoustic wave (SAW) properties of Ca₃Ga₂Ge₃O₁₄ (CGG), Sr₃Ga₂Ge₃O₁₄ (SGG) and Pb₃Ga₂Ge₃O₁₄ (PGG) crystals have been investigated. The first-principle calculations show that CGG and SGG have similar electronic structure properties, the remarkable difference between PGG and another two crystals is the absence of lower part of valence band. Both the calculated effective charges and bond populations show that there is considerable covalency between cations and O atom. The calculated SAW results show that PGG has the lowest velocities because of its highest density, SGG has the highest electromechanical coupling coefficients, CGG and SGG have more zero power flow angles and negligible diffraction angles than PGG crystal. Some promising cut-types such as Y-cut 148° of SGG, X-cut 154° of CGG and Y-cut 0° of PGG have been selected for their SAW applications.

Keywords: Ca₃Ga₂Ge₃O₁₄, Sr₃Ga₂Ge₃O₁₄, Pb₃Ga₂Ge₃O₁₄, electronic structure, surface acoustic wave

1. Introduction

Ca₃Ga₂Ge₃O₁₄ (CGG) (Belokoneva, Simonov, Butashin, Mill, & Belov, 1980; Belokoneva & Belov, 1981), Sr₃Ga₂Ge₃O₁₄ (SGG) (Kaminskii et al., 1984) and Pb₃Ga₂Ge₃O₁₄ (PGG) (Sorokin et al., 2004; Bezmaternykh, Vasil'ev, Gudim, & Temerov, 2004) crystals which all belong to langasite family (Chai, Bustamante, & Chou, 2000; Mill & Pisarevsky, 2000; Mill, 2001) exhibit excellent piezoelectric property and have been attracting more and more attention in the surface acoustic wave (SAW) application (Mill, Pisarevsky, & Belokoneva, 1999; Kludzin, Balysheva, & Smirnov, 2005). Due to their outstanding electromechanical and acoustic properties (Bungo et al., 1999), they are becoming the promising candidates to replace traditional piezoelectric material (Gualtieri, Konsiski, & Ballato, 1994)—quartz in remarkably reducing the insertion loss of SAW devices. In addition, because of their excellent thermal and chemical stability (Mill et al., 2004; Thiele & da Cunha, 2006), they can be used in various kinds of harsh circumstances, such as high temperature, acid and alkali environment.

Since CGG crystal was first synthesized in 1980s, several groups have been doing a great amount of research on it. Mill, Klimentova, Maximov, Molchanov, and Pushcharovsky (2007) have pointed out that the piezoelectric modulus d_{11} of CGG crystal increases when the size of cations forming the framework increases, especially the size of dodecahedral ions. Based on this theory, different elements can be used to substitute the cations in CGG crystals to improve its piezoelectric property (Zhou, Xu, Hua, & Fan, 2004; Takeda et al., 1999). That is the main reason why CGG, SGG, and PGG crystals present different piezoelectric properties. In addition, Kaminskii et al. (1984) and Sorokin et al. (2004) have measured the material data including elastic, piezoelectric and dielectric constants. However, as far as we know, the theoretical studies of electronic structures for CGG, SGG, and PGG crystals have not been reported yet. For the SAW applications, there is a harsh requirement (Naumenko & Solie, 2001) that the substrates of SAW devices should have low propagation velocity (v), high electromechanical coupling coefficients (k^2), zero power flow angle (PFA) and other excellent SAW properties. So it is also critical to predict the optimal cut-types which possess these merits simultaneously by theoretical calculation. Since Campbell and Jones (1968) established the well-known partial wave method to estimate optimal crystal cuts and propagation directions for excitation of piezoelectric surface waves, many research groups (Bungo et al., 1999; Naumenko & Solie, 2001; Shibayama, Yamanouchi, Sato, & Meguro, 1976; Yamanouchi, Odagawa, Kojima, & Matsumura, 1997; Yakovkin, Taziev, & Kozlov, 1995; Puccio, Malocha, Saldanha, & da Cunha, 2007) have predicated the SAW properties of various piezoelectric materials by using this method, the theoretical results

agree well with the experimental measurements (Bungo et al., 1999; Yakovkin, Taziev, & Kozlov, 1995).

This paper consists of two main parts, in the first part, by using first-principles method (Lu, Lan, Li, W. C. Wang, & C. L. Wang, 2006; Lee, Tan, & Lim, 2006; Huang, Cheng, Xue, & Li, 2014; Huang, Yang, Lu, & Gao, 2012), we investigated the electronic structures of these three crystals and make a comparison with each other. In the second part, we calculated their SAW properties in X-cut, Y-cut and Z-cut and then selected several promising cuts for their SAW applications.

2. Computational Methods

2.1 Crystal Structures and First-Principle Method

$(\text{Ca,Sr,Pb})_3\text{Ga}_2\text{Ge}_3\text{O}_{14}$ crystals have the same structures with $\text{La}_3\text{Ga}_5\text{SiO}_{14}$ (LGS)-type (Mill & Pisarevsky, 2000; Mill, 2001) which belongs to the space group $P321$ of trigonal system (Xin, Zheng, Kong, & Shi, 2008). There are four cation site types in this structure: a dodecahedral site locates at 3e position, an octahedral site (1a), a small sized tetrahedral site (2d) and a large sized tetrahedral site (3f). For CGG and SGG crystal (Kaminskii et al., 1984), Ca^{2+} and Sr^{2+} occupy the 3e position, 2d position is occupied by Ge^{4+} , 1a position and 3f position are both occupied by Ga^{3+} and Ge^{4+} . While for the PGG crystal according to Bezmaternykh et al. (2004), 1a position and 3f position are both occupied by Ge^{4+} , Ga^{3+} only occupy 2d position and Pb^{3+} occupy 3e position. According to Kaminskii et al. (1984) and Mill et al. (2007), the content of Ga^{3+} in 1a and 3f position equal to 30% and 50%. In order to conveniently investigate the electronic structure of CGG and SGG crystals, we constructed the super cells in which the occupations of Ga^{3+} and Ge^{4+} in 1a and 3f positions are equal (1:1). Figure 1 (a) shows the super-cell structures of CGG and SGG; Figure 1 (b) shows the super-cell structures of PGG crystal.

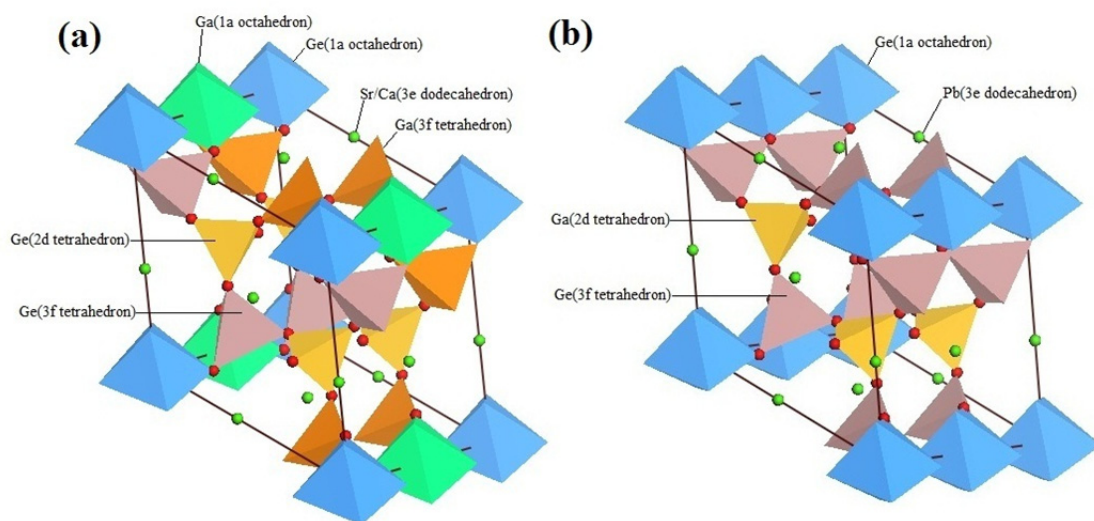


Figure 1. (a) The $1 \times 1 \times 2$ super cell of $\text{Ca}_3\text{Ga}_2\text{Ge}_3\text{O}_{14}$ and $\text{Sr}_3\text{Ga}_2\text{Ge}_3\text{O}_{14}$ crystals, (b) the $1 \times 1 \times 2$ super cell of $\text{Pb}_3\text{Ga}_2\text{Ge}_3\text{O}_{14}$ crystal

In order to obtain the ground state structures, we optimized their geometrical structures. The geometrical optimization was performed by using Broyden-Fletcher-Goldfarb-Shanno (BFGS) algorithm, the generalized gradient approximation of Perdew et al. (GGA-PBE) and ultrasoft pseudopotential are used. In these calculations, the energy cut and SCF convergence tolerance is set to 340.0 eV and 1×10^{-6} eV atom⁻¹ respectively. Local density approximation (LDA) of Ceperley and Alder (CA-PZ) and ultrasoft pseudopotential are used to calculate the band structure and density of state (DOS) and partial density of state (PDOS).

2.2 Surface Acoustic Wave Calculation Method

According to the well-known partial wave method (Campbell & Jones, 1968), the phase velocity can be obtained by solving Christoffel equation:

$$\begin{bmatrix} \Gamma_{11} - \rho v^2 & \Gamma_{12} & \Gamma_{13} & \Gamma_{14} \\ \Gamma_{12} & \Gamma_{22} - \rho v^2 & \Gamma_{23} & \Gamma_{24} \\ \Gamma_{13} & \Gamma_{23} & \Gamma_{33} - \rho v^2 & \Gamma_{34} \\ \Gamma_{14} & \Gamma_{24} & \Gamma_{34} & \Gamma_{44} \end{bmatrix} \begin{bmatrix} A_1 \\ A_2 \\ A_3 \\ A_4 \end{bmatrix} = 0 \tag{1}$$

In Equation (1), $\Gamma_{ik} = c_{ijkl}l_i l_j$ ($i, k = 1, 2, 3$), $\Gamma_{i4} = e_{kij}l_k l_j$ ($i = 1, 2, 3$), $\Gamma_{ij} = -\epsilon_{ijk}l_j l_k$ ($i = 4, j = 4$). A_i is the amplitude component, v is phase velocity, ρ is the density of crystal, l_i is the direct cosine of wave propagation direction angle γ , c , e and ϵ is elastic, piezoelectric and dielectric constant respectively. Free surface velocities (v_f) and metalized surface velocities (v_m) can be obtained by solving this Equation with the free and metalized boundary conditions at the surface of semi-infinite crystal.

Electromechanical coupling coefficient k^2 is given by

$$k^2 = 2(v_f - v_m) / v_f \tag{2}$$

Power flow angle (PFA) φ reflects the discordance between the propagation direction γ of energy flow and phase velocity:

$$\varphi = \tan^{-1} \frac{1}{v_f} \frac{dv_f}{d\gamma} \tag{3}$$

Anisotropy factor δ can reflect the SAW diffraction (the most optimal value is -1):

$$\delta = \frac{d\varphi}{d\gamma} \tag{4}$$

3. Results and Discussion

3.1 Electronic Structure

Figure 2 shows the band structures of CGG, SGG and PGG crystals. For SGG and CGG, the top of valence band and the bottom of the conduction band are in the same points, which means that they are direct band gap materials. While the band feature of PGG crystal is a little different from SGG and CGG, it presents indirect band gap feature. Their energy gap values are listed in Table 1, it can be seen SGG has the highest energy gap, while PGG has the lowest energy gap.

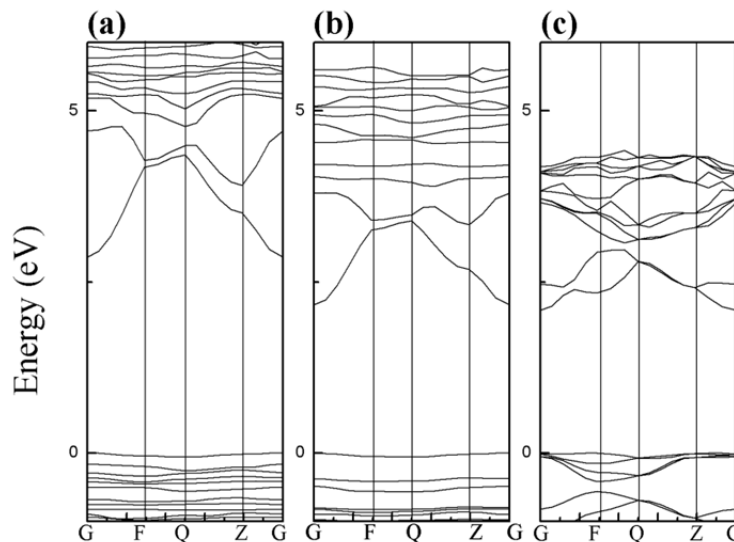


Figure 2. The band structure of SGG(a),CGG(b) and PGG(c) crystal

Table 1. The calculated energy gap of SGG, CGG and PGG

	Energy gap(eV)
CGG	2.18
PGG	2.86
SGG	2.09

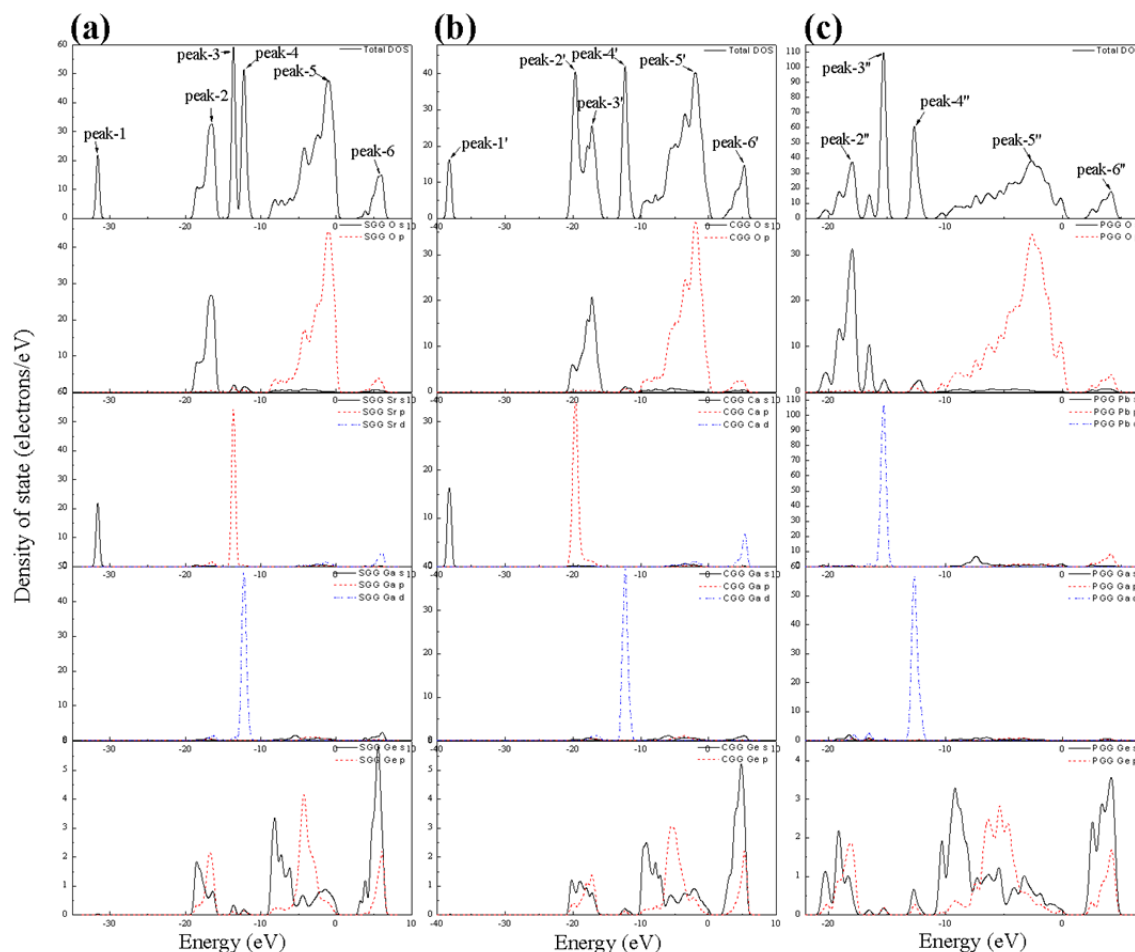


Figure 3. The total and partial density of States of SGG(a), CGG(b) and PGG(c) crystal

Figure 3 (a) shows the total density of state (TDOS) and the partial density of state (PDOS) of SGG crystal. It can be seen that the TDOS can be divided into four parts. The lower part of valence band ($-40 \text{ eV} < E < -25 \text{ eV}$) is totally dominated by Sr 5s orbitals, a sole steep peak locates at -31.64 eV (peak-1). In the middle part of the valence band ($-20 \text{ eV} < E < -10 \text{ eV}$), there are three peaks locate at -16.54 eV (peak-2), -13.65 eV (peak-3) and -12.24 eV (peak-4). Analyzing from its PDOS, it is clear to see that peak-2 is mainly composed of O 2s orbitals, Sr 4p, Ga 3d and Ge 4s, 4p orbitals also have small contribution to this region. Meanwhile, two extremely high peaks: peak-3 and peak-4, are formed by Sr 4p and Ga 3d orbitals respectively. The upper part of valence band ($-10 \text{ eV} < E < 0 \text{ eV}$) is mainly composed of O 2p orbitals which have small admixture with O 2s, Sr 4d, Ga 4s, 4p and Ge 4s, 4p orbitals, the highest peak in this part locates at -1.01 eV (peak-5). On the other hand, the contribution to conduction band mainly comes from the hybridization of the orbital of Ge, Ga, Sr and O, the highest peak in this part locates at 5.86 eV (peak-6). It can be seen from the PDOS of SGG that the states of cations and states of O are overlapped obviously at the upper parts of valence band and conduction band, which suggests that covalent bonds exist between cations and O atom.

The DOS and PDOS of CGG shown in Figure 3 (b) have the same characteristics when compared with SGG crystal. It also can be divided into four parts, where the corresponding peaks locate at -38.25 eV (peak-1'),

-19.72 eV (peak-2''), -17.21 eV (peak-3'), -12.32 eV (peak-4'), -1.95 eV (peak-5') and 5.22 eV (peak-6'). Compared with the DOS of SGG, we could find that the peaks of the valence band have a tendency of shifting to the lower energy. Moreover, Ca, Ga, Ge and O atom have the similar contribution to the whole energy band as compared with Sr, Ga, Ge, and O in SGG.

As shown in Figure 3(c), the remarkable difference between PGG and $(\text{Sr,Ca})_3\text{Ga}_2\text{Ge}_3\text{O}_{14}$ is the absence of lower part of valence band ($-40 \text{ eV} < E < -25 \text{ eV}$), which is mainly caused by Pb atom. The other corresponding peaks can also be found locating at -18.04 eV (peak-2''), -15.38 eV (peak-3''), -12.70 eV (peak-4''), -2.67 eV (peak-5'') and 4.09 eV (peak-6''). Unlike $(\text{Sr,Ca})_3\text{Ga}_2\text{Ge}_3\text{O}_{14}$, the peak-3'' is formed by Pb 5d orbitals.

Table 2. The effective charges of SGG, CGG and PGG

CGG	Charge	SGG	Charge	PGG	Charge
Ca(3e)	1.22	Sr(3e)	1.16	Pb(3e)	1.40
Ga(1a)	1.44	Ga(1a)	1.40	Ge(1a)	1.83
Ge(1a)	1.65	Ge(1a)	1.73	Ga(2d)	1.21
Ga(3f)	1.33	Ga(3f)	1.31	Ge(3f)	1.39
Ge(3f)	1.52	Ge(3f)	1.62	O	-0.91
Ge(2d)	1.54	Ge(2d)	1.63		
O	-0.89	O	-0.91		

For $(\text{Ca, Sr, Pb})_3\text{Ga}_2\text{Ge}_3\text{O}_{14}$, the formal charges of Sr, Ca, Pb, Ga, Ge and O are +2, +2, +2, +3, +4 and -2 respectively. Table 2 lists their effective charges, it can be seen that the calculated effective charges are smaller than their formal charges, which means that the bonding nature of them is not fully ionic. Table 3 lists the population of cation-O bonds, it can be seen clearly that all bond population possess positive values, which means there are considerable covalency in cation-O bonds. The strength of (Ca, Sr, Pb)-O bond are obviously smaller than that of Ga-O, Ge-O in each crystal. Besides, the bond populations of Ge-O and Ga-O in PGG crystal are larger than that in SGG and CGG.

Table 3. Bond population of cation-O in CGG, SGG and PGG

CGG	Bond population	SGG	Bond population	PGG	Bond population
Ca-O(3e)	0.15	Sr-O(3e)	0.14	Pb-O(3e)	0.20
Ga-O(1a)	0.32	Ga-O(1a)	0.33	Ge-O(1a)	0.40
Ge-O(1a)	0.36	Ge-O(1a)	0.34	Ga-O(2d)	0.56
Ga-O(3f)	0.44	Ga-O(3f)	0.48	Ge-O(3f)	0.50
Ge-O(3f)	0.39	Ge-O(3f)	0.38		
Ge-O(2d)	0.49	Ge-O(2d)	0.44		

3.2 SAW Properties

In the SAW calculation, so the choice of material constants greatly affect the calculated results (Naumenko & Solie, 2001). Table 4 lists the elastic, piezoelectric, dielectric constants and material density of CGG, SGG and PGG crystals (Kaminskii et al., 1984; Sorokin et al., 2004). By solving Christoffel equation, the phase velocity, electromechanical coupling coefficient, power flow angle and anisotropy factor of X-cut, Y-cut and Z-cut of $(\text{Sr, Ca, Pb})_3\text{Ga}_2\text{Ge}_3\text{O}_{14}$ are obtained, the results are shown in Figure 4, Figure 5, Figure 6 and Figure 7.

As shown in Figure 4, it is clear to see that most phase velocities of these crystals are less than 3000 m s^{-1} , which are lower than that of traditional piezoelectric crystals, such as quartz ($3200 \text{ m/s} \cong v \cong 3800 \text{ m/s}$) and LiNbO_3 ($3500 \text{ m/s} \cong v \cong 4000 \text{ m/s}$) (Shibayama, Yamanouchi, Sato, & Meguro, 1976; Slobodnik Jr, 1976; Kovacs, Anhorn, Engan, Visintini, & Ruppel, 1990). In these three crystals, PGG has the lowest velocities (varied from 2100 m s^{-1} to 2500 m s^{-1}) because of its highest density, which means it has the superiority of

fabricating miniaturized SAW devices. The phase velocities of CGG and SGG are varied from 2400 m s⁻¹ to 3000 m s⁻¹ and 2300 m s⁻¹ to 3100 m s⁻¹ respectively. In addition, the velocity curves of Y-cut and Z-cut have a central symmetry axis at $\gamma = 90^\circ$, while the curve of X-cut does not have this property.

Table 4. The elastic constants c_{ij} (10^{10} N m⁻²), piezoelectric constants e_{ij} (C m⁻¹), relative dielectric constants ϵ_{ij} and density ρ (g cm⁻³) of SGG, CGG and PGG crystals

Material constants	SGG ^a	CGG ^a	PGG ^b
c_{11}	15.55	15.55	14.65
c_{12}	8.16	8.67	6.69
c_{13}	7.55	7.29	7.04
c_{14}	1.78	0.95	1.02
c_{33}	20.86	23.96	18.12
c_{44}	5.60	4.55	5.21
c_{66}	3.70	3.44	3.98
e_{11}	-0.567	-0.344	-0.26
e_{14}	0.055	0.0014	0.090
ϵ_{11}	13.80	15.50	26.20
ϵ_{33}	18.21	24.22	13.90
ρ	5.087	4.589	6.884

a: Kaminskii et al., 1984; b: Sorokin et al., 2004.

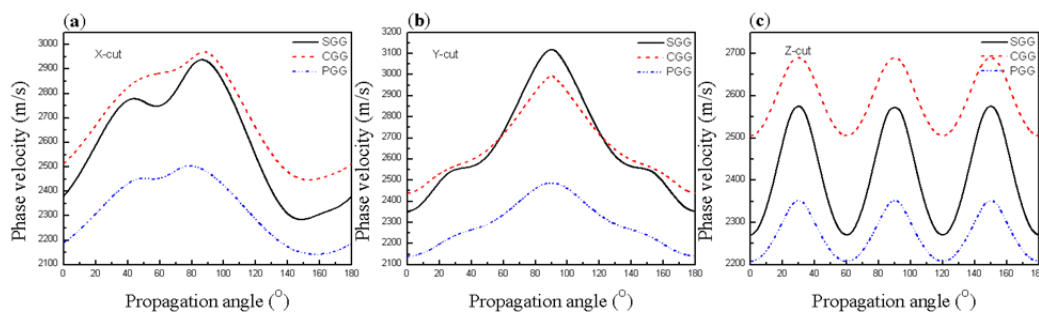


Figure 4. The phase velocities of SGG, CGG and PGG in X-cut(a), Y-cut(b) and Z-cut(c)

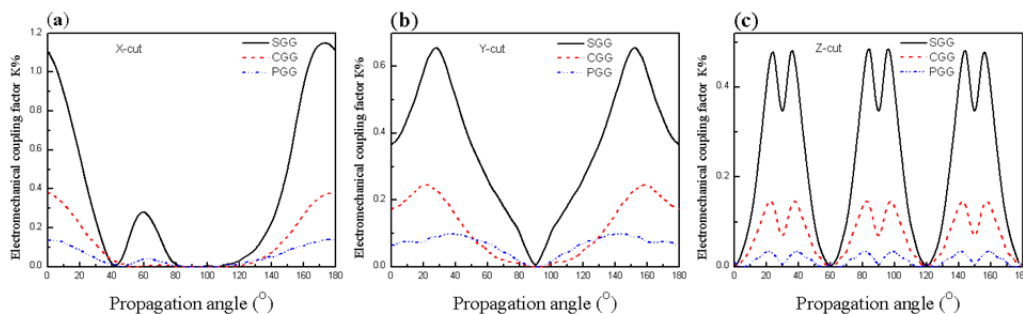


Figure 5. The electromechanical coupling coefficients of SGG, CGG and PGG in X-cut(a), Y-cut(b) and Z-cut(c)

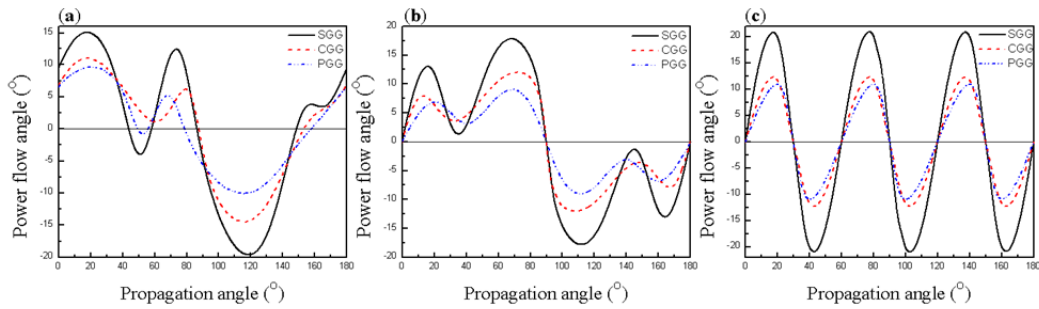


Figure 6. The power flow angles of SGG, CGG and PGG in X-cut(a), Y-cut(b) and Z-cut(c)

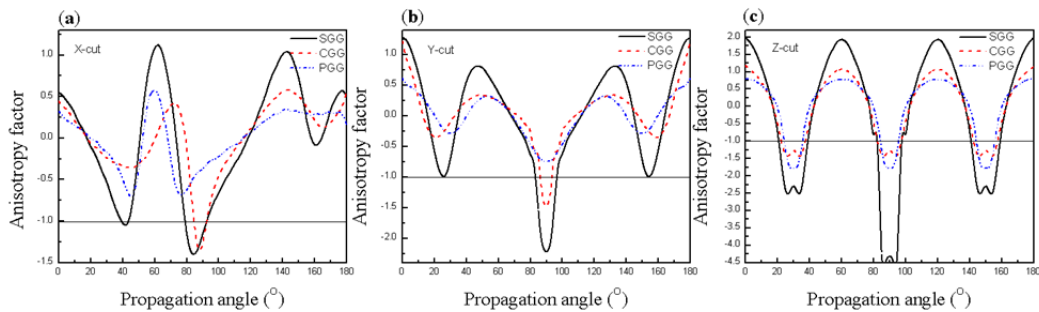


Figure 7. The anisotropy factors of SGG, CGG and PGG in X-cut (a), Y-cut (b) and Z-cut(c)

Table 5. The SAW characteristics of zero PFA cut-types

Crystal	Cut-types	Propagation angle(°)	Phase velocity (m s ⁻¹)	Electromechanical coupling coefficient	Anisotropy factor
SGG	X-cut	58	2751.34	0.27%	0.98
	X-cut	148	2282.03	0.46%	0.83
	Y-cut	0	2319.00	0.37%	1.28
	Z-cut	30	2575.74	0.35%	-2.29
	Z-cut	90	2575.74	0.35%	-4.32
CGG	X-cut	154	2447.00	0.19%	0.44
	Y-cut	0	2437.57	0.17%	1.20
PGG	X-cut	158	2139.80	0.10%	0.28
	Y-cut	0	2144.46	0.11%	0.61

Figure 5 shows the electromechanical coupling coefficients of these three crystals, it can be seen that SGG has obviously higher k^2 in each cuts, the highest values in X-cut, Y-cut and Z-cut can attain 1.15%, 0.66% and 0.48% respectively. This outstanding feature may come from its excellent piezoelectric performance (Zhou et al., 2004), especially from the contribution of large e_{11} . The k^2 of CGG and PGG are relatively lower, their highest values in X-cut, Y-cut, Z-cut are 0.38%, 0.25%, 0.15% and 0.14%, 0.10%, 0.03% respectively. In the field of design of interdigital transduce (IDT), the insertion loss of IDT is smaller if the substrate possesses larger electromechanical coupling coefficient (Lu, Zhu, Liu, Fang, & Wen, 2006). So it is reasonable to predicate that SGG can exhibit excellent performance in reducing insertion loss of devices when making SAW devices.

Figure 6 shows their power flow angles, we could see all of these three crystals have zero PFA angles, the PFA of SGG are relatively higher than that of another two crystals. In Y-cut and Z-cut, they all have three and seven zero PFA angles. While in X-cut, SGG and PGG have four zero PFA angles, CGG has only one zero PFA angles. Figure 7 shows their anisotropy factors, many propagation angles with negligible diffraction ($\delta = -1$) can be found. In Z-cut, they all have six negligible diffraction angles, while in Y-cut and X-cut, SGG and CGG have

four and two negligible diffraction angles, PGG does not have any negligible diffraction angles.

In addition, comprehensively taking account into these various properties, we list the properties of zero PFA cuts for these crystals in Table 5. As we can see, Y-cut 148° of SGG has low phase velocity (2282.03 m s⁻¹) and high electromechanical coefficient (0.46%), which exhibits superior SAW performance. Besides, Y-cut 0° and Z-cut 30° of SGG, X-cut 154° of CGG, Y-cut 0° of PGG can be given priority in the field of SAW application.

4. Conclusion

In this paper, the first-principle calculation based on density functional theory have been used to study the electronic structures of CGG, SGG and PGG crystals, their calculated energy gaps are 2.18, 2.86 and 2.09 eV respectively. By comparing the calculated results with each other, we found that CGG and SGG have similar electronic structure characteristic in TDOS spectrum, the atoms in CGG has similar contribution to the TDOS as compared with the corresponding atoms in SGG. However, the PDOS of PGG is quite different from that of another two crystals in the lower part of valence band. For these three crystals, we found that the states of cations and states of O are overlapped obviously at the upper parts of valence band and conduction band, which suggested that covalent bonds exist between cations and O atom. This property was also confirmed by the analysis of effective charges and bond population. The strength of Ga-O and Ge-O bond are obviously larger than that of (Ca, Sr, Ca)-O.

By solving the Christoffel equation with the free and metalized boundary on the surface of semi-infinite crystal, their phase velocities, electromechanical coupling coefficients, power flow angles and anisotropy factors in X-cut, Y-cut and Z-cut are obtained. By comparing the calculated SAW results with each other, we found that PGG has the lowest velocities (varied from 2100 m s⁻¹ to 2500 m s⁻¹), SGG has the highest electromechanical coupling coefficients, CGG and SGG have more zero power flow angles and negligible diffraction angles than PGG crystal. Some promising cut-types such as Y-cut 148° of SGG, X-cut 154° of CGG and Y-cut 0° of PGG were listed, which may provide theoretical guidance for their SAW application.

Acknowledgments

This work is supported by Training Program Foundation for the Talents of Beijing City (No.2012D005007000003), computational studies were performed by using the resources of Supercomputing Center of Chinese Academy of Sciences.

References

- Belokoneva, E., & Belov, N. (1981). Crystal structure of the synthetic gallium germanium gehlenite $\text{Ca}_2\text{Ga}_2\text{GeO}_7=\text{Ca}_2\text{Ga}(\text{GaGe})\text{O}_7$ and comparison with the structure of $\text{Ca}_3\text{Ga}_2\text{Ge}_4\text{O}_{14}=\text{Ca}_3\text{Ge}[(\text{Ga}_2\text{Ge})\text{Ge}_2\text{O}_{14}]$. *Soviet Physics Doklady*, 26, 931.
- Belokoneva, E., Simonov, M., Butashin, A., Mill, B., & Belov, N. (1980). Crystal structure of calcium gallogermanate $\text{Ca}_3\text{Ga}_2\text{Ge}_4\text{O}_{14}=\text{Ca}_3\text{Ge}[(\text{Ga}_2\text{Ge})\text{Ge}_2\text{O}_{14}]$ and its analog $\text{Ba}_3\text{Fe}_2\text{Ge}_4\text{O}_{14}=\text{Ba}_3\text{Fe}[(\text{FeGe}_2)\text{Ge}_2\text{O}_{14}]$. *Soviet Physics Doklady*, 25, 954.
- Bezmaternykh, L. N., Vasil'ev, A. D., Gudim, I. A., & Temerov, V. L. (2004). The growth and structure of $\text{Pb}_3\text{Ga}_2\text{Ge}_4\text{O}_{14}$ and $\text{Ba}_3\text{Ga}_2\text{Ge}_4\text{O}_{14}$ single crystals. *Crystallography Reports*, 49(2), 271-274. <http://dx.doi.org/10.1134/1.1690429>
- Bungo, A., Jian, C., Yamaguchi, K., Sawada, Y., Kimura, R., & Uda, S. (1999). Experimental and Theoretical Analysis of SAW Properties of the Langasite Substrate with Euler Angle (0°,140°,φ). *1999 IEEE Ultrasonics Symposium Proceedings*, 231-234. <http://dx.doi.org/10.1109/ULTSYM.1999.849392>
- Campbell, J. J., & Jones, W. R. (1968). A method for estimating optimal crystal cuts and propagation directions for excitation of piezoelectric surface waves. *IEEE Transactions on Sonics and Ultrasonics*, 15(4), 209-217. <http://dx.doi.org/10.1109/T-SU.1968.29477>
- Chai, B. H. T., Bustamante, A. N. P., & Chou, M. C. (2000). A new class of ordered langasite structure compounds. *Proceedings of the 2000 IEEE/EIA International Frequency Control Symposium and Exhibition*, 163-168. <http://dx.doi.org/10.1109/FREQ.2000.887346>
- Gualtieri, J. G., Konsiski, J. A., & Ballato, A. (1994). Piezoelectric materials for acoustic wave applications, *IEEE Transactions on Ultrasonics, Ferroelectrics, and Frequency Control*, 41(1), 53-58. <http://dx.doi.org/10.1109/58.265820>
- Huang, W. Q., Cheng, B. W., Xue, C. L., & Li, C. B. (2014). Comparative studies of clustering effect, electronic and optical properties for GePb and GeSn alloys with low Pb and Sn concentration. *Physica B: Condensed*

- Matter*, 443, 43-48. <http://dx.doi.org/10.1016/j.physb.2014.03.008>
- Huang, W. Q., Yang, H., Lu, G. W., & Gao, Y. N. (2012). Theoretical calculations of the Linear, Nonlinear Elastic Constants and the Grüneisen Parameters of cubic perovskites (Sr, Ba, Pb) TiO₃. *Physica B: Condensed Matter*, 411, 56-61. <http://dx.doi.org/10.1016/j.physb.2012.11.020>
- Kaminskii, A. A., Belokoneva, E. L., Mill, B. V., Pisarevskii, Yu. V., Sarkisov, S. E., Silvestrova, I. M., ... Khodzhabagyan, G. G. (1984). Pure and Nd³⁺-doped Ca₃Ga₂Ge₄O₁₄ and Sr₃Ga₂Ge₄O₁₄ single crystals, their structure, optical, spectral luminescence, electromechanical properties, and stimulated emission. *Physica Status Solidi(a)*, 86, 345-362. <http://dx.doi.org/10.1002/pssa.2210860139>
- Kludzin, V. V., Balysheva, O. L., & Smirnov, Y. G. (2005). Langasite Family Crystals for Acoustoelectronics Applications. *Wave Electronics and Its Application in Information and Telecommunication Systems*, 1-10.
- Kovacs, G., Anhorn, M., Engan, H. E., Visintini, G., & Ruppel, C. C. W. (1990). Improved material constants for LiNbO₃ and LiTaO₃. *1990 IEEE Ultrasonics Symposium Proceedings*, 435-438. <http://dx.doi.org/10.1109/ULTSYM.1990.171403>
- Lee, N. T. S., Tan, V. B. C., & Lim, K. M. (2006). First-principles calculations of structural and mechanical properties of CuSn. *Applied Physics Letters*, 88(3), 031913. <http://dx.doi.org/10.1063/1.2165280>
- Lu, G. W., Lan, J. H., Li, C. X., Wang, W. C., & Wang, C. L. (2006). Theoretical study of CCl₄ adsorption and hydrogenation on a Pt (111) surface. *The Journal of Physical Chemistry B*, 110(48), 24541-24548. <http://dx.doi.org/10.1021/jp0600054>
- Lu, W. K., Zhu, C. C., Liu, J. H., Fang, J. A., & Wen, C. B. (2006). Study of Insertion Loss for Wavelet Transform Element of New SAW Type. *Acta Electronica Sinica*, 34(2), 371-373. <http://dx.doi.org/10.3321/j.issn:0372-2112.2006.02.034>
- Mill, B. V. (2001). Two new lines of langasite family compositions, 2001 IEEE International Frequency Control Symposium and PDA Exhibition, 255-261.
- Mill, B. V., Klimenkova, A. A., Maximov, B. A., Molchanov, V. N., & Pushcharovsky, D. Yu. (2007). Enantiomorphism of the Ca₃Ga₂Ge₄O₁₄ compound and comparison of the Ca₃Ga₂Ge₄O₁₄ and Sr₃Ga₂Ge₄O₁₄ structures. *Crystallography Reports*, 52(5), 785-794. <http://dx.doi.org/10.1134/S1063774507050069>
- Mill, B. V., Maksimov, B. A., Pisarevskii, Yu. V., Danilova, N. P., Pavlovska, A., Werner, S., & Schneider, J. (2004). Phase transitions in compounds with the Ca₃Ga₂Ge₄O₁₄ structure. *Crystallography Reports*, 49(1), 60-69. <http://dx.doi.org/10.1134/1.1643965>
- Mill, B. V., & Pisarevsky, Y. V. (2000). Langasite-type materials: from discovery to present state. *Proceedings of the 2000 IEEE/EIA International Frequency Control Symposium and Exhibition*, 133-144. <http://dx.doi.org/10.1109/FREQ.2000.887343>
- Mill, B. V., Pisarevsky, Yu. V., & Belokoneva, E. L. (1999). Synthesis, growth and some properties of single crystals with the Ca₃Ga₂Ge₄O₁₄ structure. *Proceedings of the 1999 Joint Meeting of the European Frequency and Time Forum and the IEEE International Frequency Control Symposium*, 829-834. <http://dx.doi.org/10.1109/FREQ.1999.841433>
- Naumenko, N., & Solie, L. (2001). Optimal Cuts of Langasite, La₃Ga₅SiO₁₄ for SAW Devices. *IEEE Transactions on Ultrasonics, Ferroelectrics, and Frequency Control*, 48(2), 530-537. <http://dx.doi.org/10.1109/58.911736>
- Puccio, D., Malocha, D. C., Saldanha, N., & da Cunha, M. P. (2007). SAW Parameters on Y-cut Langasite Structured Materials. *IEEE Transactions on Ultrasonics, Ferroelectrics, and Frequency Control*, 54(9), 1873-1881. <http://dx.doi.org/10.1109/TUFFC.2007.471>
- Shibayama, K., Yamanouchi, K., Sato, H., & Meguro, T. (1976). Optimum cut for rotated Y-cut LiNbO₃ crystal used as the substrate of acoustic-surface-wave filters. *Proceedings of the IEEE*, 64(5), 595-597. <http://dx.doi.org/10.1109/PROC.1976.10181>
- Slobodnik A. J. Jr. (1976). Surface acoustic waves and SAW materials. *Proceedings of the IEEE*, 64(5), 581-595. <http://dx.doi.org/10.1109/PROC.1976.10180>
- Sorokin, B. P., Glushkov, D. A., Bezmaternykh, L. N., Temerov, V. L., Gudim, I. A., & Aleksandrov, K. S. (2004). Electromechanical properties of Pb₃Ga₂Ge₄O₁₄ piezoelectric crystals grown from solution in a melt. *Physics of the Solid State*, 46, 458-461. <http://dx.doi.org/10.1134/1.1687860>

- Takeda, H., Kato, T., Chani, V. I., Morikoshi, H., Shimamura, K., & Fukuda, T. (1999). Effect of (Sr, Ba) substitution in $\text{La}_3\text{Ga}_5\text{SiO}_{14}$ and $\text{La}_3\text{M}_{0.5}\text{Ga}_{5.5}\text{O}_{14}$ ($\text{M}=\text{Nb}^{5+}, \text{Ta}^{5+}$) crystals on their synthesis, structure and piezoelectricity. *Journal of Alloys and Compounds*, 290(1-2), 79-84. [http://dx.doi.org/10.1016/S0925-8388\(99\)00203-0](http://dx.doi.org/10.1016/S0925-8388(99)00203-0)
- Thiele, J. A., & da Cunha, M. P. (2006). High temperature LGS SAW gas sensor. *Sensors and Actuators B: Chemical*, 113(2), 816-822. <http://dx.doi.org/10.1016/j.snb.2005.03.071>
- Xin, J., Zheng, Y. Q., Kong, H. K., & Shi, E. W. (2008). From *ab initio* forecast of piezoelectric properties to growth of piezoelectric single crystals. *Applied Physics Letters*, 93(25), 252901. <http://dx.doi.org/10.1063/1.3025545>
- Yakovkin, I. B., Taziev, R. M., & Kozlov, A. S. (1995). Numerical and experimental investigation saw in langsite. 1995 *IEEE Ultrasonics Symposium Proceedings*, 389-392. <http://dx.doi.org/10.1109/ULTSYM.1995.495604>
- Yamanouchi, K., Odagawa, H., Kojima, T., & Matsumura, T. (1997). Theoretical and experimental study of superhigh electromechanical coupling surface acoustic wave propagation in KNbO_3 single crystal. *Electronics Letters*, 33(3), 193-194. <http://dx.doi.org/10.1049/el:19970145>
- Zhou, J., Xu, J. Y., Hua, W. X., & Fan, S. J. (2004). Bridgman growth of new piezoelectric single crystal $\text{Sr}_3\text{Ga}_2\text{Ge}_4\text{O}_{14}$. *Materials Science and Engineering: B*, 106(2), 213-217. <http://dx.doi.org/10.1016/j.mseb.2003.09.024>

Copyrights

Copyright for this article is retained by the author(s), with first publication rights granted to the journal.

This is an open-access article distributed under the terms and conditions of the Creative Commons Attribution license (<http://creativecommons.org/licenses/by/3.0/>).